JOURNAL OF SOLID STATE CHEMISTRY 96, 294–300 (1992)

High Temperature Crystal Structure and DSC of $Sn_2P_2S_6$

B. SCOTT, M. PRESSPRICH, R. D. WILLET, AND D. A. CLEARY*

Department of Chemistry, Washington State University, Pullman, Washington 99164-4630

Received April 29, 1991

We report the single crystal X-ray diffraction of $Sn_2P_2S_6$ at 110°C. The crystals are monoclinic, with space group $P2_1/n$, a = 9.362(2) Å, b = 7.493(1) Å, c = 6.550(3) Å, β = 91.17(3)°, and Z = 2. The structure consists of $P_2S_6^{-4}$ anions linked together via S–Sn contacts. Each Sn atom is coordinated to eight S atoms. The S–Sn distances range from 2.914–3.227 Å. At room temperature, $Sn_2P_2S_6$ crystallizes in the space group Pc and has a strong ferroelectric response. Using differential scanning calorimetry, the transition to the paraelectric state is determined to be 60 ± 2°C. The DSC data are also consistent with the phase transition being second order. The major change in the structure results from movement of the tin atoms. The $P_2S_6^{-4}$ units remain essentially unchanged. Neither the room temperature nor the high temperature phase exhibits a layered structure characteristic of the transition metal phosphorus chalcogenides, $M_2P_2X_6$.

Introduction

The transition metal hypodithiophosphates, $M_2P_2X_6$, where M is a transition metal and X is sulfur or selenium, were first reported by Hahn and Klingen in 1965 (*1*). Nitsche and co-workers reported the synthesis of a series of tin (and lead)–phosphorus–sulfur compounds in 1970 and 1974 (*2, 3*). One of these was $Sn_2P_2S_6$, which the authors noted crystallized in orange, transparent polyhedra. They reported the space group as Pc with lattice parameters a = 6.43 Å, b = 7.47 Å, c = 11.03 Å, β = 122.2°. In 1973, Klingen, Ott, and Hahn reported three different $Sn_2P_2S_6$ phases, one rhombohedral and two monoclinic which they labeled as monoclinic(I) and monoclinic(II) (*4*). Dittmar and Schäfer performed the room temperature single crystal structure determination of monoclinic(II) $Sn_2P_2S_6$ in 1974 and reported the space group Pn (equivalent to Pc) with space group parameters a = 9.378(5) Å, b = 7.488(5) Å, c = 6.513(5) Å, β = 91.15°(5), Z = 2 (*5*). Also in 1974, Carpentier and Nitsche described the ferroelectric behavior of $Sn_2P_2S_6$ crystals, again monoclinic(II), and concluded that the axis of polarization was along the [101] direction of the Pc cell and that the Curie temperature was 66 ± 2°C (*6*). Since then, the ferroelectric behavior of monoclinic(II) $Sn_2P_2S_6$ (and $Sn_2P_2Se_6$) has attracted considerable attention (*7–13*). Using the room temperature structural information on $Sn_2P_2Se_6$, $Pb_2P_2S_6$, and $Pb_2P_2Se_6$ (all $P2_1/n$), Carpentier and Nitsche reasoned that the ferroelectric phase transition in $Sn_2P_2S_6$ was the result of tin-pair displacements along the [101] direction. In this pa-

* To whom correspondence should be addressed.

0022-4596/92 $3.00

per, we verify the room temperature structure of monoclinic(II) $Sn_2P_2S_6$ and report the 110°C structure. Our results are consistent with the proposed displacement suggested by Carpentier and Nitsche (*6*).

Experimental Section

Materials. All of the materials used were from commercial suppliers and used as received. Tin was in the form of −20 mesh granular and was supplied by Mallinckrodt. Red phosphorus powder, amorphous, −100 mesh, was purchased from Alfa. Sulfur powder, −60 mesh, was supplied by Johnson Mathey, Inc. (USA). The resublimed iodine crystals used were from Johnson Mathey Chemicals, Limited (England). Spectrophotometric grade cyclohexane, used as a calibration standard in the DSC experiments, was from Aldrich Chemical Co. Its reported melting point is 6.5°C. High purity indium, also used as a DSC standard, was provided by the DSC manufacturer (Perkin–Elmer). Indium's melting point is 156.6°C.

Synthesis. Large crystals of $Sn_2P_2S_6$ were grown from the elements using iodine vapor transport. Stoichiometric amounts of tin, phosphorus, and sulfur (4 g total) were lightly ground together and then transferred to a quartz reaction tube (15-cm × 1.3-cm od, standard wall). Iodine crystals (0.225 g) were added to the reaction tube. (Iodine serves as the transporting agent.) The sample was evacuated, sealed, and placed in a Marshall tube furnace. The growth zone of the tube was set to 700°C for 1 day to allow reverse transport out of the growth zone. After that, the growth zone was lowered to 600°C and the sample zone was raised to ≈630°C. After 4 days, a good yield of large $Sn_2P_2S_6$ crystals was realized. The size of the crystals appeared to be limited by the inside diameter of the reaction tube. From the batch, small crystals (orange/yellow, transparent) suitable for single crystal X-ray diffraction experiments were selected.

X-ray diffraction. A thin yellow plate of the title compound with dimensions 0.08 × 0.25 × 0.31 mm was mounted on a thin glass fiber. The X-ray reflection data were collected on a Syntex $P2_1$ diffractometer upgraded to Nicolet R3 specifications (*14*). Graphite monochromatized MoK_α (λ = 0.71069 Å) radiation was used. A preliminary room temperature determination agreed well with the previous work of Dittmar and Schäfer (*5*). The crystal was then heated to 110°C employing a method described previously (*15*). The orientation matrix and lattice parameters were optimized from a least-squares calculation on 25 carefully centered reflections with high Bragg angles. This resulted in a monoclinic unit cell with a = 9.362(2) Å, b = 7.493(1) Å, c = 6.550(3) Å, β = 91.17(3)°, V = 459.6(3) Å^3, Z = 2, ρ = 3.55 g cm^{-3}. The intensities of 1682 reflections were measured ($2\theta_{max}$ = 60°C) using an ω scan (0.85° range) with speeds varying from 4–29.3° min^{-1}. Three standard reflections ($\bar{4}\,3\,1$, $1\,\bar{1}\,0$, 600) were monitored every 96 reflections and showed no systematic variation. Following data reduction, 1215 reflections remained, with 1054 having $|F| \geq 3\sigma(F)$. R for equivalent reflections was 0.0233. The space group, determined from systematic absences, was found to be $P2_1/n$ (#14). The positions of all atoms were found via direct methods. All atoms were refined anisotropically to a final R = 0.0567, R_w = 0.0658, and g = 0.0018. The functions minimized were

$$R = \sum \frac{||F_o| - |F_c||}{|F_o|} \quad (1)$$

$$R_w = \sqrt{\left[\frac{\sum w(|F_o| - |F_c|)^2}{\sum w|F_o|^2}\right]}, \quad (2)$$

where $w = 1/[\sigma^2(F) + g(F)^2]$. An absorption coefficient of 70.3 cm^{-1} was calculated, and empirical absorption corrections (laminar) yielded a transmission range of 0.369–0.898. All data reduction, including

Lorentz and polarization corrections, structure solution and refinement, and graphics were performed with SHELXTL 5.1 software (*16*).

Characterization. Differential scanning calorimetry (DSC) was performed on a Perkin–Elmer DSC7 interfaced to a Perkin–Elmer Delta Series computer. DSC is used to determine the ferroelectric transition temperature of $Sn_2P_2S_6$. A sample of powdered $Sn_2P_2S_6$ (19.6 mg) was heated at a rate of 20.0°C/min. Indium (reported mp 156.6°C) and cyclohexane (reported mp 6.54°C) served as calibration standards. The sample and the standards were run using liquid nitrogen as a heat sink. A slow helium gas purge improved the thermal conductivity between the sample pans and the heat sink.

The Raman spectrum of powdered $Sn_2P_2S_6$ was recorded on a spectrometer which is based on an Instruments SA double 1-m monochromator having holographic gratings. The 514.5-nm line of an argon ion laser was used for excitation. The laser radiation was passed through a Pellin Brocha prism monochromator and then focused onto the sample. The scattered radiation was collected by a lens and admitted to the monochromator. The light output of the monochromator was converted to an electrical signal by a Hamamatsu R2949 photomultiplier, and single-photon events were counted with a Stanford Research SR 400 photon counter. The monochromator drive and photon counter were controlled by an 80206 based computer. The wavenumber scale is accurate to ±2 cm^{-1}, and the displayed spectrum was taken with 2-cm^{-1} resolution. The data reported resulted from the addition of several scans. The powdered $Sn_2P_2S_6$ showed no signs of laser damage at the conclusion of the experiment.

Results and Discussion

The ferroelectric phase transition appears as a very broad transition in DSC, see Fig. 1, with a peak at 60°C. A conservative estimate of the uncertainty of this peak is ±2°. Under similar experimental conditions, the observed melting point of cyclohexane (7.7 mg) was 6.68°C, and the observed melting point of indium (4.7 mg) was 155.6°C. As already mentioned, Carpentier and Nitsche reported a phase transition temperature of 66°C using differential thermal analysis (DTA).

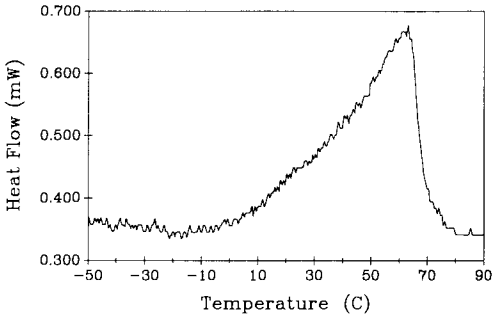

FIG. 1. DSC curve for powdered $Sn_2P_2S_6$. The peak occurs at 60°C.

The shape of the DSC curve is characteristic of a classical second-order continuous phase transition (*17*). In a first-order phase transition, the heat capacity goes to infinity since the input of heat, Δq, results in no temperature change, ΔT:

$$C = \frac{\Delta q}{\Delta T}. \tag{3}$$

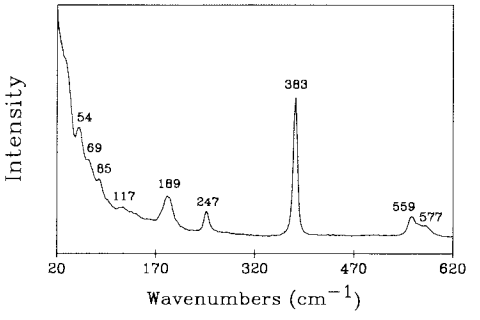

FIG. 2. Room temperature Raman spectrum of powdered $Sn_2P_2S_6$.

The ordinate in Fig. 1 is equivalent to the heat capacity, C_p, plus a constant. Hence, in a first-order phase transition, such as the melting of indium, one should observe a peak, the integral of which is equal to the enthalpy of transition:

$$\Delta H_{trans} = \int C_p dt. \quad (4)$$

In a second-order phase transition, the heat capacity does not diverge, but rather undergoes a discontinuous jump, similar to what is observed in Fig. 1. The second-order nature of the transition is consistent with the fact that the low temperature space group, *Pn*, is a maximal subgroup of the high temperature space group, $P2_1/n$. The high temperature crystal structure reported here was done at 110°C, well above the completion of the phase transition. The nature of this phase transition remains under investigation.

The Raman spectrum of powdered $Sn_2P_2S_6$ is shown in Fig. 2. It is consistent with that reported by Gurzan *et al.*(*18*). It is also similar to the Raman spectra of $Fe_2P_2S_6$, $Co_2P_2S_6$, and $Ni_2P_2S_6$ reported by Sourisseau *et al.* (*19*). In that work, peaks above 150 cm^{-1} have been assigned to the $P_2S_6^{-4}$ group, and those below 150 cm^{-1} have been assigned to modes involving the metal ions. The intense band at 383 cm^{-1} is assigned as the symmetric valence mode $\nu_s(PS_3)$. The absence of any unexpected bands is taken as assurance that the compound is reasonably pure.

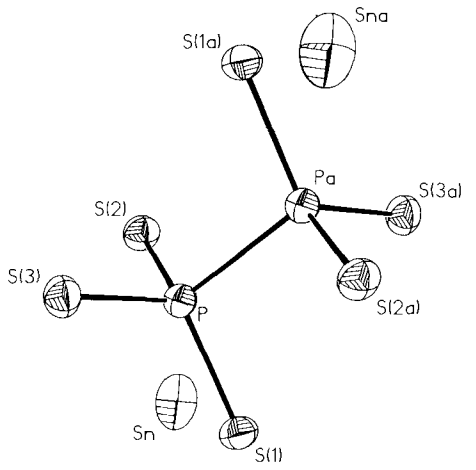

FIG. 3. A diagram of the $Sn_2P_2S_6$ unit at 110°C showing thermal ellipsoids. The center inversion is at the midpoint of the P–P bond.

X-ray. A diagram of the $Sn_2P_2S_6$ structure at 110°C is shown in Figure 3. Atomic coordinates and isotropic thermal parameters are listed in Table I. Bond angles and distances are listed in Table II. The $P_2S_6^{-4}$ anion sits on a center of inversion, with a P–P distance of 2.213(3) Å. The P–P distance in the corresponding room temperature structure is 2.211(9) Å. The P–S distances in the 110°C structure are 2.021(2) Å, 2.033(2) Å, and 2.035(2) Å. These agree well with the room temperature P–S distances of 2.017(7) Å, 2.025(10) Å, 2.029(10) Å, 2.032(10) Å, 2.035(10) Å, and 2.039(11) Å. The bond

TABLE I

ATOMIC COORDINATES (× 10^4) AND ISOTROPIC THERMAL PARAMETERS (Å^2 × 10^3) FOR $Sn_2P_2S_6$ AT 110°C

Atom	x	y	z	U^a
Sn	2431(1)	3692(1)	−411(1)	56(1)
S(1)	2629(2)	4975(2)	3991(3)	31(1)
S(2)	−328(2)	3090(2)	1772(3)	28(1)
S(3)	570(2)	1976(2)	6558(3)	29(1)
P	671(2)	3914(2)	4394(3)	23(1)

[a] The equivalent isotropic U is defined as one-third of the trace of the orthogonalized U_{ij} tensor.

angles about the P atom in the 110°C structure range from 103.9(1) to 115.7(4)°. The room temperature bond distances and angles are from the structure carried out in this work. These values were used for completeness, since the same crystal was used for the 110°C structure. These values agree well with those reported previously by Dittmar and Schäfer (*5*). This close resemblance of bonding geometries between the two structures indicates a rigid $P_2S_6^{-4}$ species.

The $P_2S_6^{-4}$ anions are tied together via S–Sn contacts. This connectivity results in an eight-fold coordination sphere of sulfur atoms about each Sn atom (Fig. 4a), which may be roughly described as a bicapped trigonal prism. There are two inequivalent Sn sites in the room temperature structure; one is seven coordinate with an additional contact of just over 3.5 Å, while the other is eight coordinate (Fig. 4b). Upon conversion to the 110°C structure (Fig. 4a), all the Sn atoms occupy crystallographically equivalent eight-fold coordination sites. As can be seen in Fig. 4c, the S and P atoms occupy essentially the same positions in both structures, with only the Sn atoms showing a

TABLE II

BOND LENGTHS (Å) AND BOND ANGLES (°) FOR $Sn_2P_2S_6$ AT 110°C

Atoms	Distance	Atoms	Angle
Sn–S(1)	3.042(2)	S1–Sn–S2	69.3(1)
Sn–S(2)	3.014(2)	S1–Sn–S(1*b*)	90.0(1)
Sn–S(1*b*)^{iii}	2.937(2)	S1–Sn–S(2*b*)	93.6(1)
Sn–S(2*b*)^{ii}	3.227(2)	S1–Sn–S(2*c*)	131.2(1)
Sn–S(2*c*)^{iv}	3.122(2)	S1–Sn–S(3*b*)	144.5(1)
Sn–S(3*b*)^{i}	2.914(2)	S1–Sn–S(3*c*)	86.8(1)
Sn–S(3*c*)^{iii}	3.191(2)	S1–Sn–S(3*d*)	67.5(1)
Sn–S(3*d*)^{iv}	3.225(2)	S2–Sn–S(1*b*)	71.9(1)
S(1)–P	2.021(2)	S2–Sn–S(2*b*)	73.6(1)
S(2)–P	2.035(3)	S2–Sn–S(2*c*)	143.7(1)
S(3)–P	2.033(2)	S2–Sn–S(3*b*)	75.2(1)
P–P(*a*)^{ii}	2.213(2)	S2–Sn–S(3*c*)	137.6(1)
		S2–Sn–S(3*d*)	124.7(1)
		S(1*b*)–Sn–S(2*b*)	141.4(1)
		S(1*b*)–Sn–S(2*c*)	78.0(1)
		S(1*b*)–Sn–S(3*b*)	77.7(1)
		S(1*b*)–Sn–S(3*c*)	145.0(1)
		S(1*b*)–Sn–S(3*d*)	75.3(1)
		S(2*b*)–Sn–S(2*c*)	124.7(1)
		S(2*b*)–Sn–S(3*b*)	77.2(1)
		S(2*b*)–Sn–S(3*c*)	73.6(1)
		S(2*b*)–Sn–S(3*d*)	140.7(1)
		S(2*c*)–Sn–S(3*b*)	79.1(1)
		S(2*c*)–Sn–S(3*c*)	78.1(1)
		S(2*c*)–Sn–S(3*d*)	63.7(1)
		S(3*b*)–Sn–S(3*c*)	121.9(1)
		S(3*b*)–Sn–S(3*d*)	137.5(1)
		S(3*c*)–Sn–S(3*d*)	71.4(1)

Note. Symmetry Codes: (i) x, y, z; (ii) $-x, -y, -z$; (iii) $\frac{1}{2} - x, \frac{1}{2} + y, \frac{1}{2} - z$; (iv) $-\frac{1}{2} + x, -\frac{1}{2} - y, -\frac{1}{2} + z$.

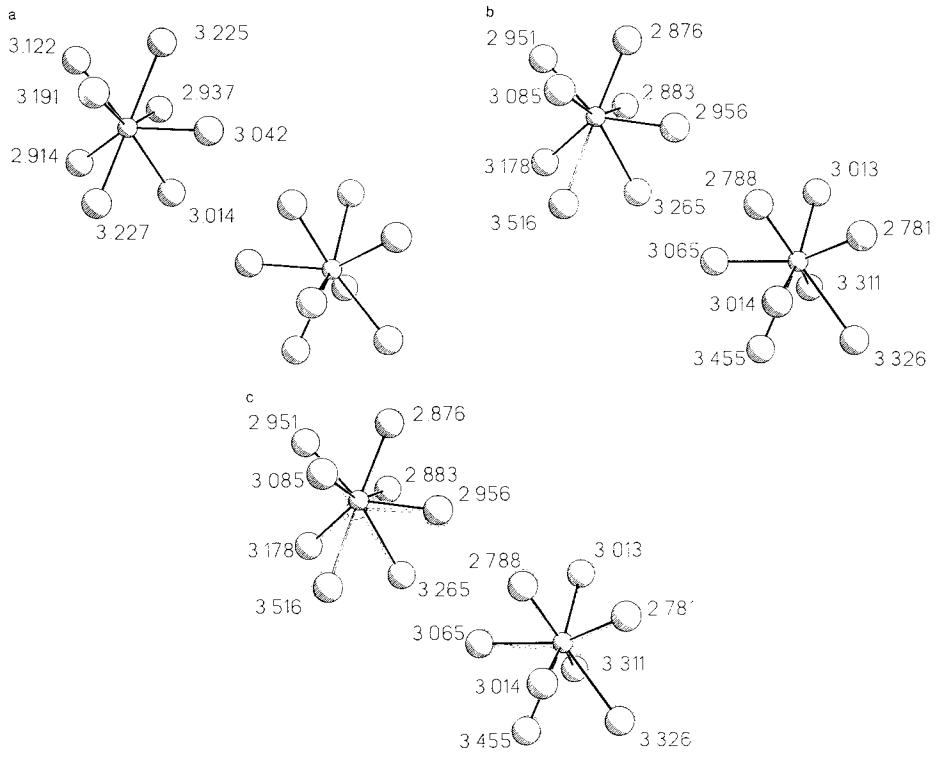

FIG. 4. A diagram of the Sn coordination spheres in the (a) 110°C phase, (b) room temperature phase, and (c) both phases overlayed. The two Sn atoms in each diagram correspond to the two Sn atoms in Fig. 3; the two P atoms have been omitted for clarity. All three diagrams are views from the same direction within the crystal.

significant shift. In the 110°C structure, the pairs of Sn atoms are related by centers of inversion. This symmetry element is lost in the room temperature structure. This movement of the Sn atoms results in a center of inversion in the 110°C structure. The two inequivalent Sn atoms thus obtained have moved 0.32(5) Å (0.30(5) Å along *a*, 0.04(4) Å along *b*, and 0.09(4) Å along *c*) and 0.22(5) Å (0.22(5) Å along *a*, 0.04(4) Å along *b*, and 0.03(3) Å along *c*), respectively. The Sn–Sn distances are 8.690 Å and 8.727 Å in the room and 110°C structures, respectively. These displacements of the Sn atoms are mainly along the [100] direction of the *Pn* space group, which is in agreement with the displacement suggested by Carpentier and Nitsche (*6*). (Note that they used the equivalent *Pc* space group for the room temperature $Sn_2P_2S_6$ structure, hence they propose the distortion to be along [101].) The displacements are consistent with a localization of the Sn(II) lone pair of electrons in the region of the long Sn–S distances. (It should be noted, however, that such an elongation has been observed in compounds without a lone pair (*20*).) In the high temperature structure, two-fold disorder of the lone pair appears to exist, leading to two relatively long Sn–S bonds (3.225 and 3.227 Å) and a concomitant elongation of the thermal ellipsoid of the Sn atom. It is anticipated that

these Sn displacement vectors will serve as an order parameter for the suspected second-order phase transition.

Conclusions

We report the 110°C single crystal structure of $Sn_2P_2S_6$. This compound is ferroelectric at room temperature (space group Pn) and undergoes a structural phase transition at 60°C to a nonferroelectric phase (space group $P2_1/n$). Using DSC, we have characterized this phase transition as being potentially second-order. The phase transition can be envisioned as movement of the Sn atoms within a rigid $P_2S_6^{-4}$ framework such that in the 110°C phase they become related by a center of inversion.

Acknowledgments

Acknowledgment is made to the Boeing Co. and NSF, through grant CHE-8408407, for the purchase of the X-ray diffractometer system.

References

1. H. Hahn and W. Klingen, *Naturwissenschaften* **52,** 494 (1965).
2. R. Nitsche and P. Wild, *Mater. Res. Bull.* **5,** 419 (1970).
3. C. D. Carpentier and R. Nitsche, *Mater. Res. Bull.* **9,** 401 (1974).
4. V. W. Klingen, R. Ott, and H. Hahn, *Z. Anorg. Allg. Chem.* **396,** 271 (1973).
5. G. Dittmar and H. Schäfer, *Z. Naturforsch.* **29b,** 312 (1974).
6. C. D. Carpentier and R. Nitsche, *Mater. Res. Bull.* **9,** 1097 (1974).
7. Ye. D. Rogach, E. A. Savchenko, D. N. Sandzhiew, N. P. Protsenko, and A. I. Rodin, *Ferroelectrics* **83,** 179 (1988).
8. J. Grigas, V. Kalesinskas, S. Lapinskas, and M. I. Gurzan, *Phase Transitions* **12(3),** 263 (1988).
9. V. Valevicius, V. Samulionis, and V. Skritskii, *Ferroelectrics* **79,** 225 (1988).
10. J. Grigas, V. Kalesinskas, S. Lapinskas, and W. Paprotny, *Ferroelectrics* **80,** 225 (1988).
11. S. S. Mitra, *Indian J. Phys.* **62A(4),** 323 (1988).
12. T. K. Barsamian, S. S. Khasanov, V. Sh. Shekhtman, Yu. M. Vysochanskii, V. Yu. Slivka, *Ferroelectrics* **67(1),** 47 (1986).
13. S. A. Flerova, O. E. Bochkov, A. Yu. Kudzin, and Yu. D. Krokhmal, *Ferroelectrics* **45(1–2),** 131 (1982).
14. C. F. Campana, D. F. Shepard, and W. M. Litchman, *Inorg. Chem.* **20,** 4039 (1981).
15. M. Pressprich, Ph. D. Thesis, Washington State University, Pullman, Washington, 99164-4630 1990.
16. G. M. Sheldrick, "SHELXTL Users Manual," Revision 5.1, Nicolet XRD Corporation, Madison, Wisconsin (1986).
17. P. W. Atkins, "Physical Chemistry," p. 186, W. H. Freeman & Co., San Francisco (1978).
18. M. I. Gurzan, A. P. Buturlakin, V. S. Gerasimenko, N. F. Korda, and V. Yu. Slivka, *Sov. Phys. Solid State Engl. Transl.* **19(10),** 1794 (1977).
19. C. Sourisseau, J. P. Forgerit, and Y. Mathey, *J. Solid State Chem.* **49,** 134 (1983).
20. G. Denes, J. Pannetier, and J. Lucas, *J. Solid State Chem.* **33,** 1 (1980).